Study of Forced Convection Heat Transfer with Single phase and mixture phase Nanofluid Model at different Reynolds Numbers

Mir Moniruzzaman Mobin[1], MD Minal Nahin[2]

[1](Dept. of Mechanical Engineering, Bangladesh University of Engineering and Technology, Bangladesh)
[2](Dept. of Mechanical Engineering, Indiana University–Purdue University Indianapolis, USA)

Abstract: *In this study, forced convection heat transfer of nanoliquids is done using both single-phase and mixture-phase models and the results are compared with experimental results. The governing equations of the study here are discretized using the finite volume method. Hybrid differencing scheme is used to calculate the face values of the control volumes. A code is written using SIMPLER algorithm and then solved using the MATLAB engine. The mixture-phase model studied here, considers two slip mechanisms between nanoparticle and base-fluid, namely Brownian diffusion and thermophoresis. Al_2O_3-water nanofluid is used for the study of nanofluid and the study shows significant increase in convective heat transfer coefficient while the mixture-phase model demonstrates slightly lower values than the single-phase model. The study is done with various nanoparticle concentrations and Reynolds numbers. With increasing particle concentration and Reynolds number, the convective heat transfer coefficient increases and as well as the shear stress. For low concentrations of the nanoparticle, Nusselt number is slightly lower than the base fluid and as the concentration increases, the Nusselt number also rises higher than the base fluid.*

Keywords - *Nanofluid, single-phase, mixture-phase, convective heat transfer, shear stress, nanoparticle volume fraction.*

I. Introduction

Conventional heat transfer fluids, such as water, engine oil, ethylene glycol etc. have very limited convective heat transfer coefficient. Maxwell [1] showed the possibility of increasing thermal conductivity of a mixture by introducing more solid particles in a fluid. Following the Maxwell's work, numerous theoretical [2-3] and experimental studies [4-5] were done with suspended solid particles in fluids and gases. These mixtures demonstrate a considerable increase of heat transfer coefficient. Because of the technological developments of the recent years, nano-sized particles are now being used with fluids which are called nanofluids.

Choi [6] studied the enhancement of thermal conductivity enhancement by suspending nanoparticles. Nanofluid is a mixture of fluid and very fine sized particles of size in the range of 1-100nm. Early researchers have worked mostly on determination of effective thermal conductivity and viscosity of nanofluids [7-10]. Masuda et al. [11] reported an increase in thermal conductivity of liquid suspensions of γ-Al_2O_3, SiO_2 and TiO_2 nanoparticles. Lee et al. [12] studied the thermal conductivity enhancement of various metal oxide suspensions. They found that the thermal conductivity of the nanofluids may increase by about 20% more than the base fluid for a very little volume fraction of nanoparticles (say 1-5%). These enhancements depend mainly on the nanoparticle size and form, volume concentration, thermal properties of both constituents etc. Correlations were developed for effective conductivity and viscosity for various nanofluids as a function of base fluid properties and volume fraction of nanoparticles. Das et al. [13] experimentally studied the temperature dependence of thermal conductivity of nanofluids. Kakaç et al.[14] summarized the important published articles on forced convection heat transfer of nanofluids. Research works on fluid flow and convective heat transfer of nanofluids in forced and free convection flows were reviewed by [15-17].

Numerical works on nanofluids are performed using two models: the single-phase model and the two-phase model. In the single-phase model, the basic hypothesis is that the nanofluid behaves like a single-phase fluid with enhanced thermo-physical properties due to the inclusion of nanoparticles. Maïga et al. [18] investigated the laminar forced convection flow of nanofluids considering a system of uniformly heated tube and another system of parallel, coaxial and heated disks. Among the two nanofluids studied, Ethylene Glycol–Al_2O_3nanofluid appears to offer a better heat transfer enhancement than water–Al_2O_3nanofluid. Demir et al. [19] studied forced convection flows of nanofluidsusing TiO_2–water and Al_2O_3–water nanofluids in a horizontal tube with constant wall temperature. In the two-phase model, different factors resulting from nanoparticle immersion such as gravity, Brownian diffusion, thermophoresis, sedimentation, dispersion etc. are considered. Two-phase models can be Eulerian-Eulerian, Eulerian-Lagrangian, mixture model etc. [20-22].Behzadmehr et al. [20] used a two-phase mixture model to investigate the turbulent convection with nanofluids in a circular tube. They found two-phase results are more precise than the homogenous modeling (single-phase) by comparing the results with

experimental ones. Bianco et al. [21]studied forced convection of nanofluids in a circular pipe using both single and mixture model. They found a maximum difference of 11% in the average heat transfer coefficient between the single and two phase model. Kalteh et al. [22, 23] studied the forced convection heat transfer of nanofluids. Buongiorno [24] theoretically developed a mixture model by considering slip mechanisms that can produce a relative velocity between the nanoparticles and the base fluid. The slip mechanisms considered were inertia, Brownian diffusion, diffusiophoresis, thermophoresis, fluid drainage, Magnus effect, and gravity. Brownian diffusion and thermophoresis were the only important slip mechanisms in nanofluids and based on the result, Buongiorno proposed a two-component four-equation non-homogeneous equilibrium model for nanofluids. Allahyari et al. [25] investigated the mixed convection of alumina-water nanofluid in an inclined tube which is heated at the top half surface.Sidik et al. [26] studied the thermal performance of fins cooled either by water or alumina-water nanofluid in a channel by lattice Boltzmann method.

Wen and Ding [27] had performed an experimental study of the convection heat transfer of nanofluids in the entrance region under laminar flow conditions. They found considerable enhancement of convection heat transfer and it was much higher than that of solely for the enhancement of thermal conduction. Heris et al. [28] studied the convective heat transfer of alumina-water nanofluid. They found much higher heat transfer coefficient than the prediction of single phase correlation. Aqueous suspensions of TiO_2 and CNT nanofluids were studied experimentally by [29, 30] to investigate the heat transfer and flow behaviors. Significant enhancement of the convective heat transfer was observed which depends on the Reynolds number, CNT concentration and the pH value. Chen et al. [31] studied the heat transfer and flow behaviors of aqueous suspensions of titanate nanotubes. They found much higher convective heat transfer coefficient, which is not merely for the enhancement of thermal conductivity. Moraveji and Esmaeili [32] did comparison between single-phase and two-phases CFD modeling of laminar forced convection flow of nanofluids in a circular tube under constant heat flux.

Nanofluids are fluids with immersed nanoparticles in it. It demonstrates much higher convective heat transfer coefficient than conventional working fluids. The present article studies the forced convection heat transfer of nanofluids using both single-phase and mixture-phase models of nanofluids. For the mixture model, the study uses the one given by Boungiorno [24]. The study focuses on the variation of convective heat transfer coefficient, Nusselt number, wall shear stress etc. with Reynolds number for various nanoparticle volume fractions. The study also discusses the volume fraction distribution of the nanoparticles.

II. Mathematical Modeling

Fluid flow and Heat transfer consists of continuity, momentum and energy equations. Some assumptions are made to simplify the governing equations. The assumptions are as following: 1. Incompressible flow 2. Axi-symmetric study 3. Steady-state flow 4. No external forces 5. Dilute solution ($\varphi \leq 0.05$) 6. Temperature independent properties.

2.1. Governing equations:

The governing equations of the mixture model are different than the single-phase model. The governing equations of the single-phase model are:

Continuity equation:

$$\nabla . (\boldsymbol{u}) = 0 \tag{1}$$

Momentum equation:

$$\rho \boldsymbol{u}. \nabla \boldsymbol{u} = -\nabla p + \mu \nabla^2 \boldsymbol{u} \tag{2}$$

Energy equation:

$$\rho c_p [\boldsymbol{u}. \nabla T] = k \nabla^2 \mathrm{T} \tag{3}$$

The governing equations of the mixture model contain equations (1) and (2) of the single-phase model. The energy equation of the mixture model is as following:

Energy equation:

$$\rho c_p [\boldsymbol{u}. \nabla T] = k \nabla^2 \mathrm{T} + \rho_{np} c_{np} \left[D_B \nabla \varphi . \nabla T + D_T \frac{\nabla T . \nabla T}{T} \right] \tag{4}$$

The two additional terms on the right side of equation (4) comes due to the heat transfer by virtue of nanoparticle diffusion. In the equation,ρc_p is the heat capacity of the nanofluid and $\rho_{np} c_{np}$ is the heat capacity of the nanoparticle.

The mixture model includes another equation which is the nanoparticle continuity equation. The equation is as following:

Continuity equation for nanoparticle:

$$\boldsymbol{u}.\nabla\varphi = \nabla.\left[D_B\nabla\varphi + D_T\frac{\nabla T}{T}\right] \tag{5}$$

Here, D_B represents the Brownian diffusion coefficient, given by the Einstein-Stokes's equation, and D_T represents the thermophoretic diffusion coefficient of the nanoparticles.

$$D_B = \frac{k_B T}{3\pi\mu d_{np}}$$

$$D_T = \left(\frac{0.26k}{2k + k_{np}}\right)\left(\frac{\mu}{\rho}\right)\varphi$$

here, k_B is the Boltzmann constant, d_{np} is particle diameter, k and k_{np} are the conductivities of the base fluid and nanoparticle respectively.

2.2. Boundary Conditions:
A circular tube of length 1.5 m and inner diameter of 13.5 mm is taken for the study. The fluid is assumed to have a uniform axial velocity V_0, and temperature T_0 (=293 K) profiles at the tube inlet section. At the exit section, the fully developed conditions are applied, which means all axial derivatives are zero. On the tube wall, no-slip and uniform heat flux boundary conditions are applied. For the mixture model, boundary conditions are also needed for the nanoparticle volume fraction. At inlet, uniform volume fraction and at wall, zero nanoparticle mass flux boundary conditions are applied. At outlet, axial derivative of volume fraction is assumed zero. The different thermo-physical properties are calculated at temperature T_0. Both the flow and thermal fields are assumed axi-symmetric.

2.3. Thermo-Physical Properties
The thermo-physical properties used in this study are calculated using the following equations.
The nanofluid density is the average of the nanoparticle and base fluid densities:

$$\rho_{nf} = \varphi\rho_{np} + (1-\varphi)\rho_{bf} \tag{6}$$

where, the subscripts *nf, p* and *bf* refer to the nanofluids, nanoparticles and base fluid respectively.
The effective specific heat of nanofluid can be calculated by the following equation as reported in [9, 18].

$$c_{nf} = \varphi c_{np} + (1-\varphi)c_{bf} \tag{7}$$

Different researchers have studied to calculate the effective viscosity of different nanofluids [11, 12]. Nguyen et al. [33] proposed the following correlation for Al_2O_3-water nanofluid as given in equation (8).

$$\mu_{nf} = 0.904e^{14.82\varphi}\mu_{bf} \tag{8}$$

Various correlations by different researchers can be found for the effective conductivity of different nanofluids [9, 11, 28]. The thermal conductivity given by Pak and Cho [9] for Al_2O_3-water nanofluid is used in this study which can be correlated as follows:

$$k_{nf} = k_{bf}(1 + 7.47\varphi) \tag{9}$$

Table 1: Thermo-physical properties of Al_2O_3 and water

Thermo-physical Properties	Al_2O_3	Water
$\rho\ [kg/m^3]$	3880	998.2
$c_p\ [J/kg.K]$	733	4182
$\mu\ [kg/m.s]$	---	9.93e-4
$k\ [W/m.K]$	36	0.597

III. Numerical Modeling

In this study, finite volume method is used to discretise the governing equations of single-phase and mixture models of the nanofluid. For discretizing, the physical space is divided into many small sub-domains which are called control volumes or cells. The shape of the cells is taken rectangular which is known as structured grids. The partial differential equations are recast on these cells and approximated by the nodal values or central values of the control volumes. Hybrid differencing scheme is used to calculate the cell face values from the cell node values. Staggered grids are used during the storing of the variables. Iterative solution strategy of SIMPLER algorithm is used to deal with non-linearity and pressure-velocity linkage of the flow

equations. Grid independence test is performed and 160 and 80 nodes in the axial and radial direction are found satisfactory for the study.
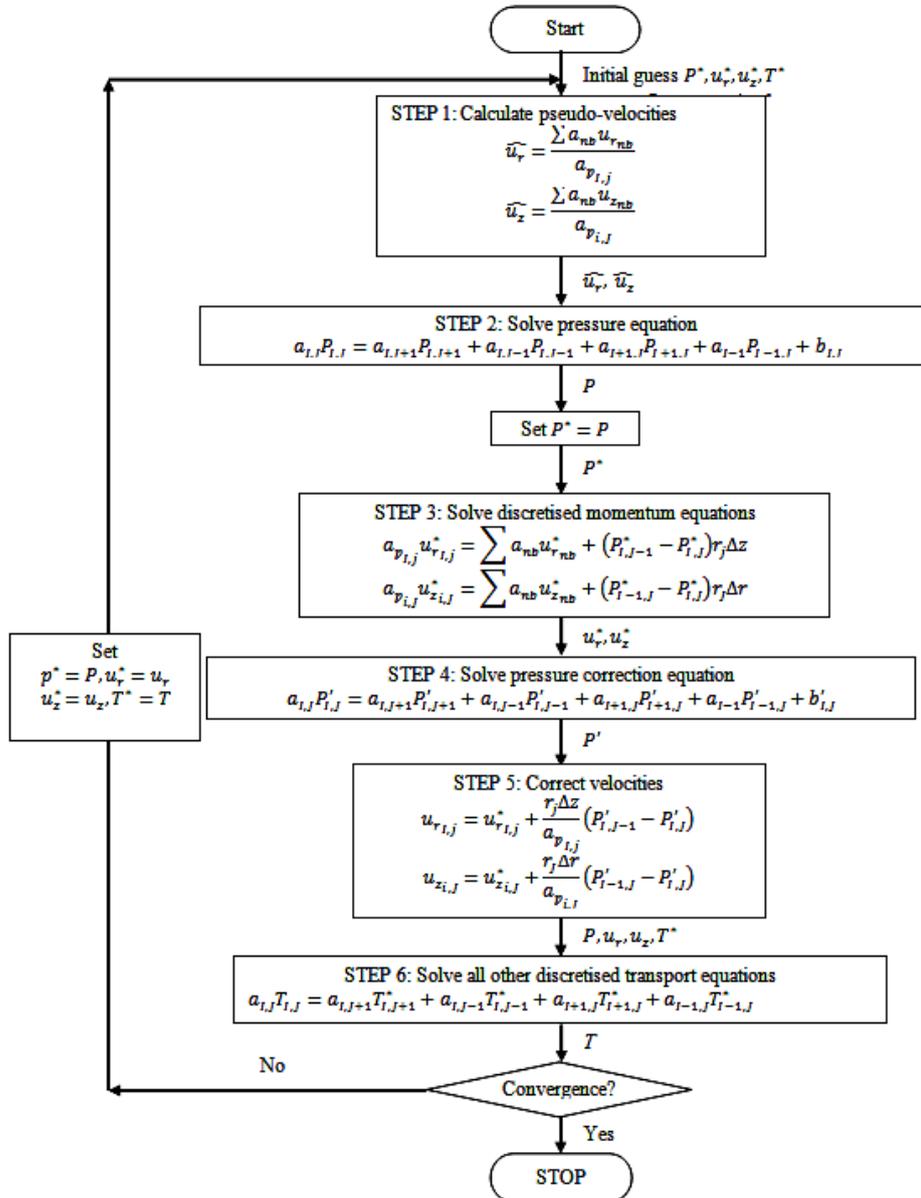

Fig 1: Flowchart of SIMPLER algorithm

The following equations are used to calculate the various parameters:

Wall shear stress:

$$\tau_s = -\mu \frac{d\,u_z}{dr}$$

Average wall shear stress:

$$\tau_{s\,av} = \frac{1}{L} \int_0^L \tau_s dz$$

Local convective coefficient:

$$h_z = \frac{q}{T_{s_z} - T_{b_z}}$$

Average convective coefficient:

$$h_{av} = \frac{1}{L} \int_0^L h_z dz$$

Local Nusselt number:

$$Nu_z = \frac{h_z D}{k}$$

Average Nusselt number:

$$Nu_{av} = \frac{h_{av} D}{k}$$

Average velocity:

$$V_{av} = \frac{2}{R^2} \int_0^R Vr dr$$

Bulk temperature:

$$T_{b_z} = \frac{2}{V_{av} R^2} \int_0^R T_z V r \, dr$$

3.1. Code Validation:

The nanofluid study is done by writing a code using FVM method. To validate the code, Nusselt numbers calculated from pure water flow is compared with the Nusselt number correlation for constant wall heat flux given by Shah and London [34]. The two results are plotted in Fig. 1. The two plots are almost identical with present results slightly higher in the developing flow region and it gradually decreases to slightly lower values in the fully developed region than the Shah and London [34] results. The above trend of variation of the present results can be attributed to the use of temperature independent properties. The Shah and London correlation is given by equation (10).

$$Nu_{z_*} = \begin{cases} 3.302 z_*^{-1/3} - 1.00 & z_* \leq 0.00005 \\ 1.302 z_*^{-1/3} - 0.50 & 0.00005 < z_* \leq 0.0015 \\ 4.364 + 8.68(10^3 z_*)^{-0.506} e^{-41z_*} & z_* > 0.0015 \end{cases} \quad (10)$$
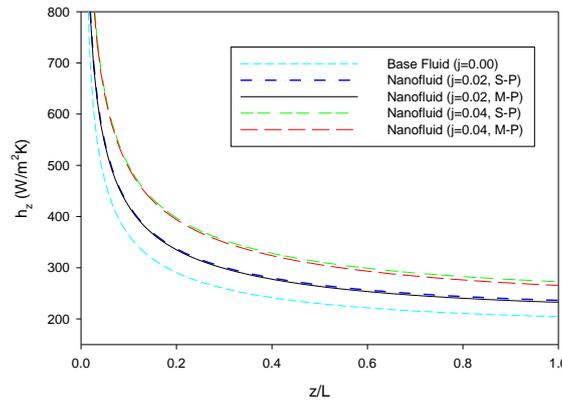
where, $z_* = \dfrac{z/D}{Re.Pr}$

Fig. 2: Code validation of nanofluid study

IV.   Results and Discussions

Simulation for nanofluidflow in the circular tube is carried out with nanoparticle volume fraction, $\varphi = 0\%, 2\%$ and 4% at three different Reynolds numbers of 200, 400 and 600. A uniform heat flux of 2500 W/m^2 is considered during the study. Change of different parameters like convective heat transfer coefficient, Nusselt number, shear stress etc. are investigated for nanoparticle immersion to the base fluid.

Fig. 3(a) shows the profiles of axial velocity along pipe radius at different length sections for pure water at Reynolds number of 200. The plot shows that for z/L=0.2 and 0.3, the two graphs almost coincide i.e. the flow is fully developed at z/L=0.2. Fig. 3(b) shows the axial velocity profiles for various nanoparticle concentration at z/L=0.3 for the mixture model. The velocity profiles are fully developed and are nearly identical with very small increase near the wall. The velocity of the mixture model slightly increases near the wall because of the reduced viscosity near the wall. The viscosity reduces near the wall because of the reduced nanoparticle concentration near the wall.
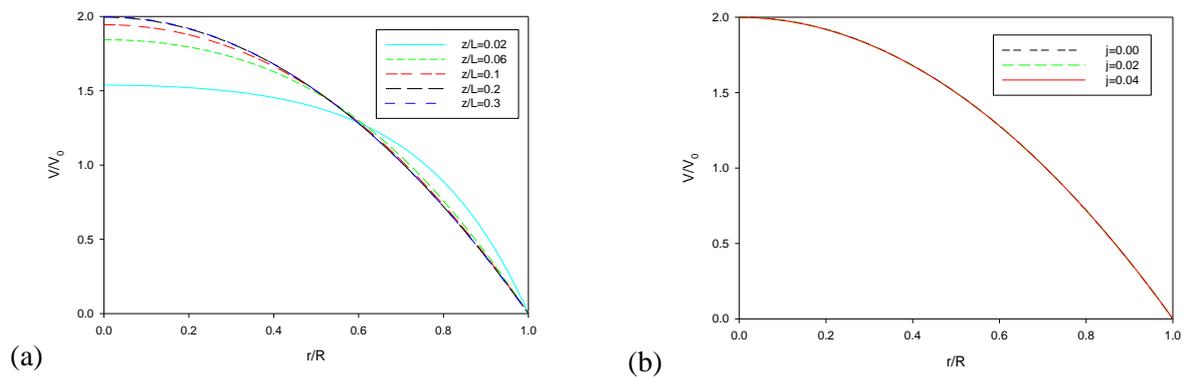
Fig. 3**:** Axial velocity profiles (a) at various locations for pure water, (b) at z/L=0.3 for various nanoparticle volume concentration.

Dimensionless temperature is plotted along pipe radius in Fig. 4(a) at various locations along the axial direction at Re=200. Thermal entrance length is larger length than the hydrodynamic entrance length. The plots for z/L=0.4, 0.7, and 1.0 are almost identical, meaning a thermally fully developed flow. Fig. 4(b) shows the dimensionless temperature at outlet for various volume concentrations. The plots are almost identical. With the increase of volume concentration, Prandtl number increases only slightly. As a result, not much variation is seen in the plots of dimensionless temperature.
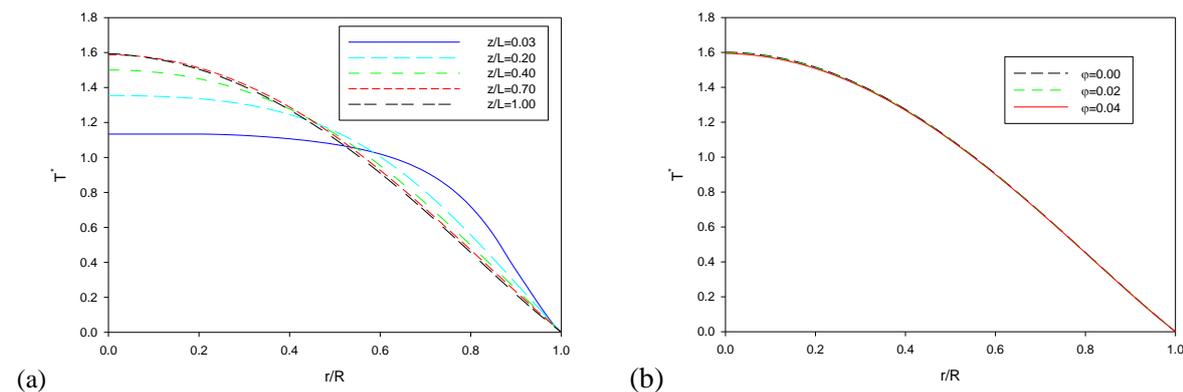

Fig. 4: Dimensionless temperature (a) at various locations for pure water, (b) at z/L=1.0 for various volume concentration.

The local convective heat transfer coefficient is plotted in Fig. 5(a) for various nanoparticle concentrations at Re=200. The S-P and M-P stands for single-phase and mixture-phase respectively. The plots show an increasing convective heat transfer coefficient with increasing particle concentration. The single-phase and the mixture-phase models provide almost same results for most of the pipe length. Towards the end of the pipe, the difference between the single-phase and mixture-phase model increases whereas mixture-phase model provides lower values. At the exit section, the increment is 15% for single-phase model and 13% for mixture-phase model for nanoparticle volume fraction of 2%. For volume fraction of 4%, the increment is 31% for single-phase and 26% for mixture-phase model. The mixture model shows lower increment in heat transfer coefficients than the single-phase model. This is because the nanoparticle volume fraction reduces near the wall and as a result thermal conductivity gets reduced near the wall. Because of the reduced particle concentration, velocity increases slightly near the wall but not enough to compensate for the reduced conductivity. Also, the two additional terms in the right side of mixture-phase energy equation is very small to make noticeable difference in the convective coefficient. Fig. 5(b) and Fig. 5(c) show the plots of local convective heat transfer coefficient for Reynolds numbers of 400 and 600. It is seen that the plots have shown almost similar trend of Fig. 5(a). Finally, the average convective heat transfer coefficient for various nanoparticle concentration and Reynolds number is plotted in Fig. 5(d). The figure shows that the convective coefficient increases with Reynolds number and nanoparticle volume fraction. The difference in the convective coefficient of single-phase and mixture-phase decreases with the Reynolds number. The average convective coefficient increases by about 35% for 4% volume fraction of nanofluid found by single-phase model of study.
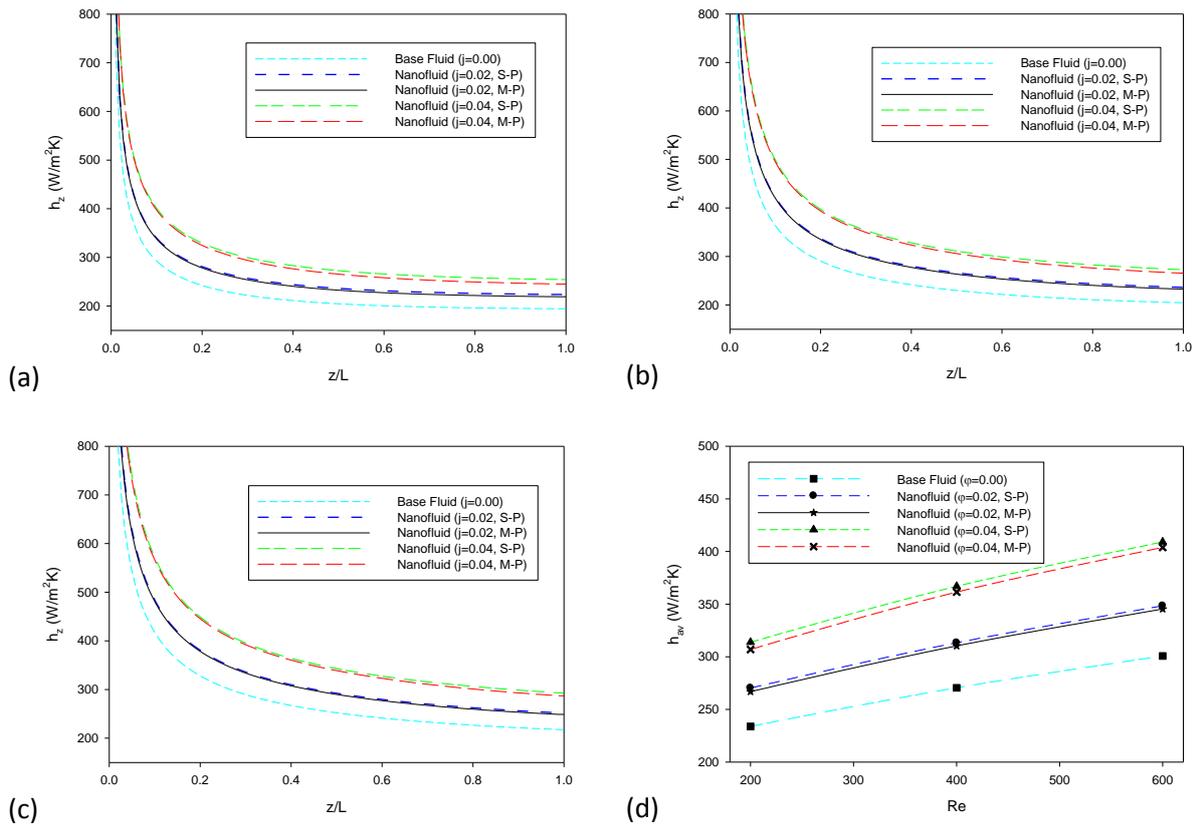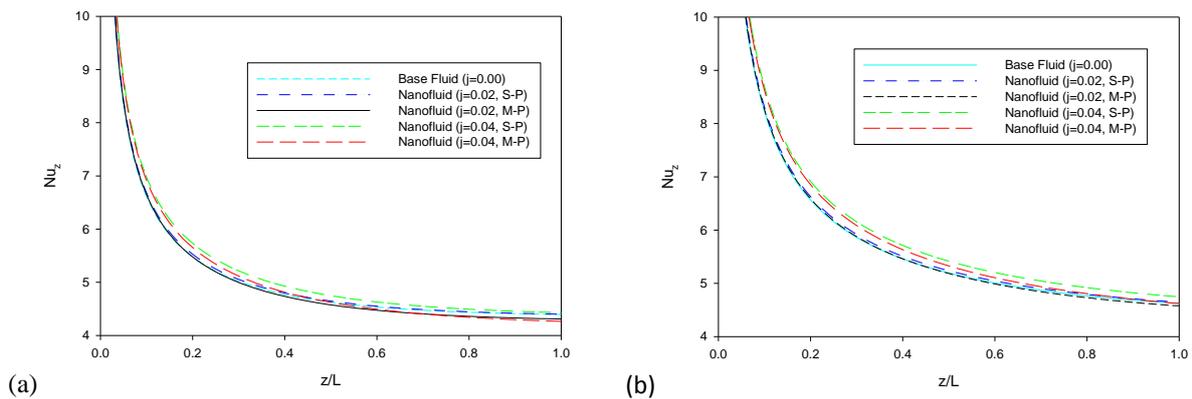
Fig. 5:convective heat transfer coefficient for various volume fractions at (a)Re=200 (b) Re=400 (c) Re=600 (d) different nanoparticle volume fractions at different Re

The local Nusselt numbers are plotted in Fig. 6(a), Fig. 6(b) and Fig. 6(c) for Reynolds numbers of 200, 400 and 600 respectively. All these graphs have the same trend as that of the convective heat transfer coefficient. The Nusselt numbers of different nanofluids depend on the nanofluid model and the nanoparticle concentration. Fig. 6(a) shows that, for mixture model study, the Nusselt number is higher in the entrance region and it falls below the Nusselt number of base fluid in the developed region. The single-phase model gives slightly higher Nusselt number than the base fluid in all sections of the pipe.
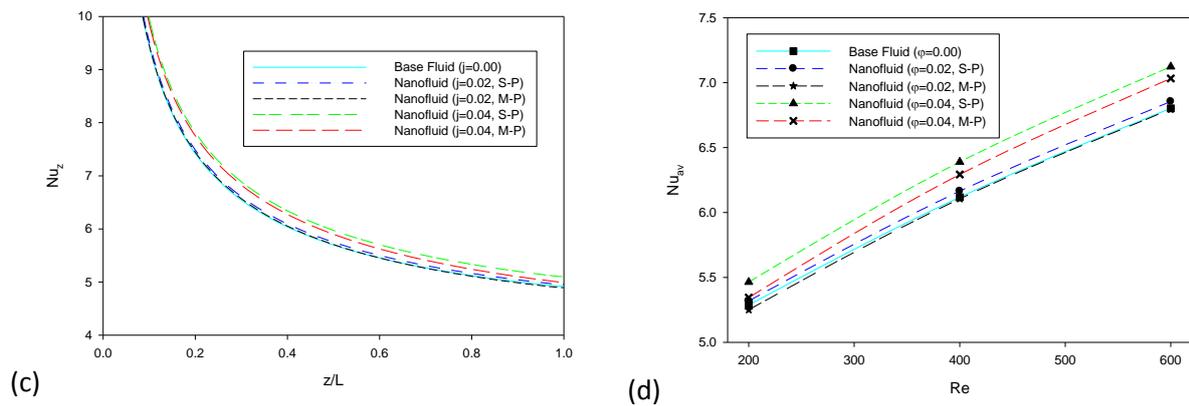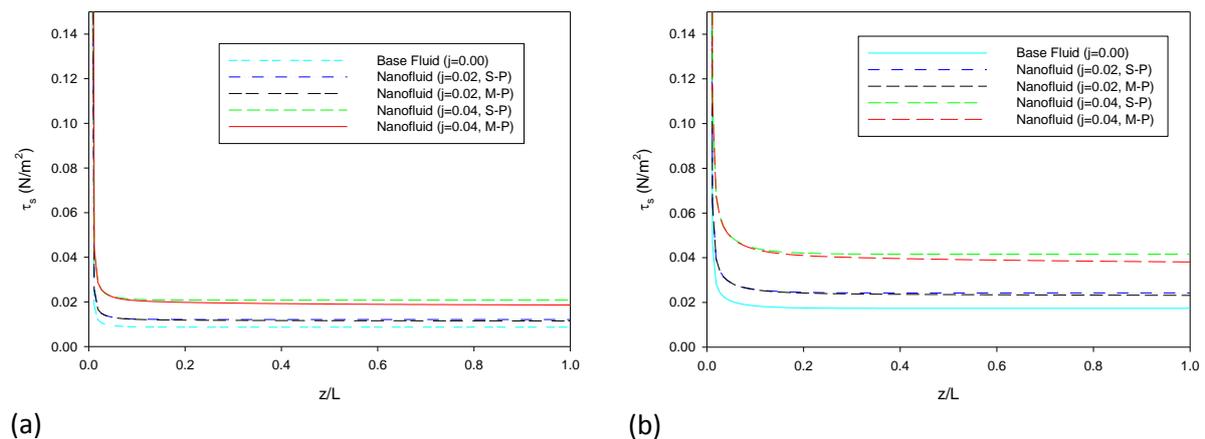
Fig. 6: Local Nusselt number for various volume fractions at (a)Re=200 (b) Re=400 (c) Re=600 (d) different nanoparticle volume fractions at different Re

The average Nusselt number is plotted in Fig. 6(d) for various nanoparticle volume fractions at different Reynolds numbers. The variation of average Nusselt number is very small with the nanoparticle volume percentages. For 2% volume fraction of nanoparticle, the mixture-phase model gives slightly lower average Nusselt number while the single-phase model gives slightly higher average Nusselt number than the base fluid. For 4% volume fraction, both the single-phase and mixture-phase model gives higher average Nusselt number than the base fluid.

The local shear stress is plotted for different volume concentration at Reynolds number of 200, 400 and 600 in Fig. 7(a), Fig. 7(b) and Fig. 7(c) respectively. The plots show that the stress drastically drops to an almost constant value near the inlet section. The shear stress is almost constant at later sections of the pipe. The shear stress increases with nanoparticle volume fraction and the relative increment with respect to base fluid is higher for 4% volume fraction than 2% volume fraction of nanoparticles. The mixture-phase model gives lower values of shear stress than the single-phase model as the viscosity near the wall reduces in the mixture-phase model. The average shear stress is plotted in Fig. 7(d) for various volume fractions at different Reynolds numbers. The average shear stress increases with Reynolds number at an almost constant rate. The average shear stress increases by 40% and 140% than the base fluid for 2% and 4% volume fraction of nanoparticles for single-phase study. For mixture-phase study, the increment is 35% and 124% for 2% and 4% volume fraction of nanoparticles respectively. As both the velocity and effective viscosity of the nanofluid increases with the nanoparticle volume fraction, the relative increment of wall shear stress increases with the increase in nanoparticle volume fraction as found in Fig. 7(d).
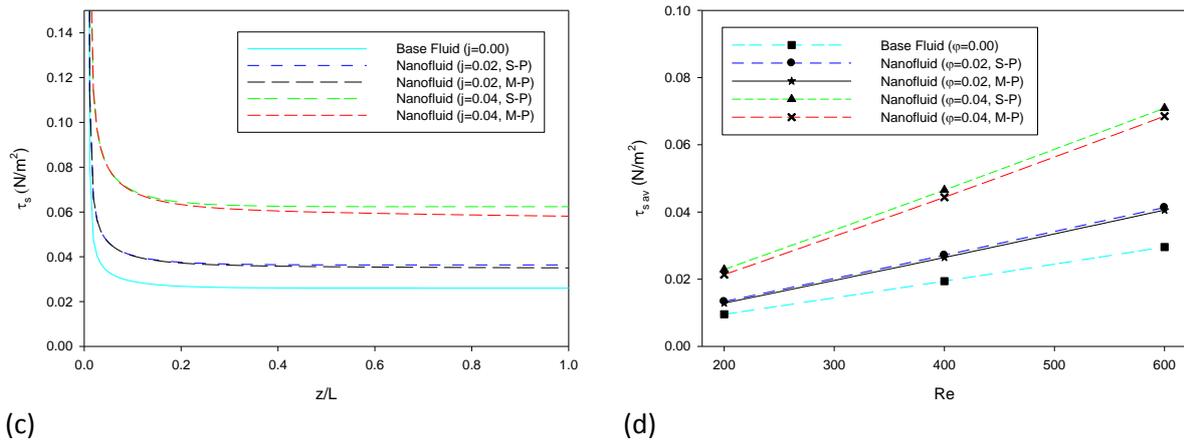
(c)   (d)

Fig. 7: Local shear stress for various volume fractions at (a) Re=200 (b) Re=200 (c)Re=200 (d) different nanoparticle volume fractions at different Re

The various average values of convective heat transfer coefficient, Nusselt number, wall shear stress etc. are given in table 2 for different volume fractions at different Reynolds numbers. The radial distribution of the nanoparticle volume fractions at inlet, middle and outlet section of the pipe are plotted in Fig. 8(a). The nanoparticle volume fraction reduces near the wall as the length of the tube increases and it is lowest near the outlet wall. The figure also shows that the volume fraction slightly increases near the axis of the pipe. Fig. 8(b) shows the distribution of nanoparticle volume fraction for different Reynolds number at the outlet section. It shows that the volume fraction near the wall is lowest for Re=200 and the value increases as the Reynolds number increases to 600. So, with higher Reynolds number, the nanoparticle distribution becomes more uniform. Both the figures are plotted for a volume fraction of 4%.

Table 2: Various average values of convective coefficient, Nusselt number and shear stress

Reynolds number	Nanoparticle volume fraction		Convective coefficient, h_{av} (W/m^{2}K)	Nusselt number, Nu_{av}	Shear stress, τ_s $_{av}*10^3$ (N/m^2)
Re=200	φ=0.00		233.9	5.29	9.54
	φ=0.02	Single-phase	270.4	5.32	13.34
		Mixture-phase	266.9	5.25	12.87
	φ=0.04	Single-phase	313.8	5.46	22.88
		Mixture-phase	307.0	5.34	21.35
Re=400	φ=0.00		270.5	6.12	19.40
	φ=0.02	Single-phase	313.3	6.16	27.12
		Mixture-phase	310.3	6.11	26.46
	φ=0.04	Single-phase	367.0	6.39	46.52
		Mixture-phase	361.4	6.29	44.39
Re=600	φ=0.00		300.8	6.80	29.57
	φ=0.02	Single-phase	348.4	6.85	41.33
		Mixture-phase	345.4	6.79	40.57
	φ=0.04	Single-phase	409.1	7.12	70.89
		Mixture-phase	403.9	7.03	68.49

(a)   (b)
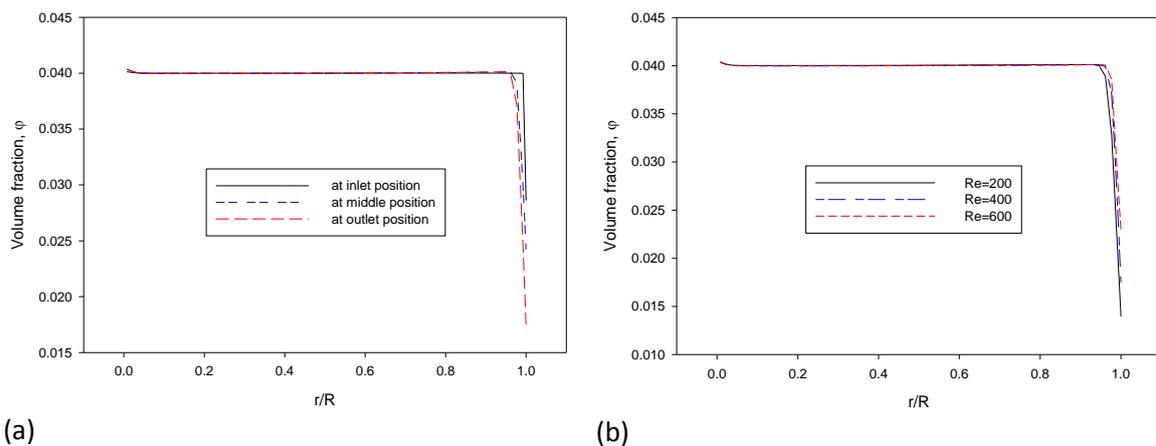
Fig. 8: Nanoparticle volume fraction at (a) different positions for Re=400 (b) at various Reynolds number

In Fig. 9, convective coefficient ratios from the present study are compared with the experimental results given by Heris et al. [28]. In the figure, convective coefficient ratio of nanofluid and base fluid are plotted against Peclet number. The nanofluid volume fraction is taken as 2.5%. The experimental convective coefficient ratio initially decreases and then increases with the Peclet number. The convective coefficient ratio found from single-phase study remains almost constant with Peclet number with very slight reduction with the increase of Peclet number. The convective coefficient ratio from the mixture-phase model slightly increases with the Peclet number. While the results from the single-phase and mixture-phase models are very close, these values are lower than the results reported by Heris et al. [28].
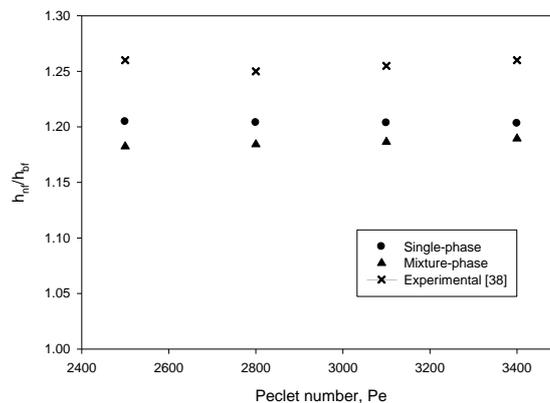

Fig. 9**:** Comparison of convective heat transfer coefficient ratio of nanofluid and base fluid for different study models.

As the numerical study model of nanofluids is still in its development, researchers have considered this range of deviation acceptable for the nanofluid study and implemented the results in calculation of the thermal performance of various heat exchanging devices. Based on the available nanofluid numerical models, the current results can be considered satisfactory for numerical study of nanofluids.

V. Conclusions

In the present study, the hydrodynamic and thermal behaviors of Al_2O_3-water nanofluid are studied in a circular tube by using single-phase and mixture-phase models. The following conclusions can be made from the study of Al_2O_3-water nanofluid.

- Convective heat transfer coefficient increases significantly with nanoparticle volume fraction for the same Reynolds number. The increment is higher for single-phase model than the mixture-phase model of Buongiorno [24]. The convective coefficient also increases with the Reynolds number.
- Nusselt number varies slightly with the nanoparticle volume fraction for the same Reynolds number. For lower values of volume fraction, the mixture-phase model gives slightly lower values of Nusselt number than the base fluid, while for higher volume fraction, Nusselt number is higher than the base

fluid. The single-phase study demonstrates slightly higher Nusselt number than base fluid both for lower and higher volume fraction. Nusselt number also increases with the Reynolds number.

- The wall shear stress increases with the nanoparticle volume fraction. The increment rate tends to increase towards higher volume fraction of nanoparticle. The mixture-phase model gives lower values of shear stress than the single-phase model.

The mixture-phase model gives the nanoparticle distribution in the flow domain. Nanoparticle concentration tends to reduce near the wall and the reduction increases towards the outlet section. The reduced volume fraction near the wall inevitably causes the reduced heat transfer coefficient than that found by the single-phase model.

References

[1]. Maxwell, J.C., A Treatise on Electricity and Magnetism, *second ed., pp. 435-441, Oxford University Press, Cambridge, 1904*

[2]. Jeffrey, D.J., Conduction through a random suspension of spheres, *Proceedings of the Royal Society of London, Series A 335, pp. 355–367 (1973).*

[3]. Xuan, Y., and Li, Q., Heat transfer enhancement of nanofuids, *Int. J. Heat Fluid Fl., vol. 21, pp. 58-64, 2000.*

[4]. Boothroyd, R.G., and Haque, H., Fully developed heat transfer to a gaseous suspension of particles flowing turbulently in duct of different size, *J. Mech. Eng. Sci., vol. 12 (3), pp. 191–200, 1970.*

[5]. Sohn, C.W., and Chen, M.M., Microconvective thermal conductivity in disperse two-phase mixtures as observed in a low velocity couette flow experiment, *J. Heat Transfer, vol. 103, pp. 45–51, 1981.*

[6]. Choi, S.U.S., Enhancing thermal conductivity of fluids with nanoparticles, developments and applications of non- Newtonian flows, D. A. Siginer and H. P. Wang (eds.*), ASME, FED-vol. 231, MD-vol. 66, pp. 99-105, 1995.*

[7]. Ding, Y., Alias, H., Wen, D., and Williams, R.A., Heat transfer of aqueous suspensions of carbon nanotubes (CNT nanofluids), *Int. J. Heat Mass Tran., vol. 49, pp. 240–250, 2006.*

[8]. He, Y., Jin, Y., Chen, H., Ding, Y., Cang, D., and Lu, H., Heat transfer and flow behaviour of aqueous suspensions of TiO_2 nanoparticles (nanofluids) flowing upward through a vertical pipe, *Int. J. Heat Mass Tran., vol. 50, pp. 2272–2281, 2007.*

[9]. Pak, B. C., and Cho, Y., Hydrodynamic and heat transfer study of dispersed fluids with submicron metallic oxide particles, *Exp. Heat Transfer, vol. 11, pp. 151–170, 1998.*

[10]. Xuan, Y., and Li, Q., Heat transfer enhancement of nanofluids, *Int. J. Heat Fluid Fl., vol. 21, pp. 58–64, 2000.*

[11]. Masuda, H., Ebata, A., Teramae, K., and Hishinuma, N., Alteration of thermal conductivity and viscosity of liquid by dispersing ultrafine particles (Dispersion of γ-Al_2O_3, SiO_2 and TiO_2 Ultra-Fine Particles), *NetsuBussei (in Japanese), vol. 4 (4), pp. 227–233, 1993.*

[12]. Lee, S., Choi, S.U.S., Li, S., and Eastman, J.A., Measuring thermal conductivity of fluids containing oxide nanoparticles, *J. Heat Transfer, vol. 121, pp. 280–289, 1999.*

[13]. Das, S.K., Putra, N., Thiesen, P., and Roetzel, W., Temperature dependence of thermal conductivity enhancement for nanofluids, *J. Heat Transfer, vol. 125, pp. 567–574, 2003.*

[14]. Kakaç, S., and Pramuanjaroenkij, A., Review of convective heat transfer enhancement with nanofluids, Int. *J. Heat Mass Tran., vol. 52, pp. 3187–3196, 2009.*

[15]. Wang, X.Q., and Mujumdar, A.S., Heat transfer characteristics of nanofluids: a Review, *Int. J. Therm. Sci., vol. 46, pp. 1–19, 2007.*

[16]. Wang, X.Q., and Mujumdar, A.S., A Review on nanofluids - Part II: Experiments and applications, Braz. *J. Chem. Eng., vol. 25, no. 04, pp. 631 - 648, 2008.*

[17]. Chandrasekar, M., Suresh, S., and Senthilkumar, T., Mechanisms proposed through experimental investigations on thermophysical properties and forced convective heat transfer characteristics of various nanofluids – a Review, *Renew. Sust. Energ. Rev., vol. 16, pp. 3917– 3938, 2012.*

[18]. Maïga, S.E.B., Palm, S.J., Nguyen, C.T., Roy, G., and Galanis, N., Heat transfer enhancement by using nanofluids in forced convection Flows, *Int. J. Heat Fluid Fl., vol. 26, pp. 530–546, 2005.*

[19]. Demir, H., Dalkilic, A.S., Kürekci, N.A., Duangthongsuk, W., and Wongwises, S., Numerical investigation on the single phase forced convection heat transfer characteristics of TiO_2 nanofluids in a double-tube counter flow heat exchanger, *Int. Commun. Heat Mass, vol. 38, pp. 218–228, 2011.*

[20]. Behzadmehr, A., Saffar-Avval, M., and Galanis, N., Prediction of turbulent forced convection of a nanofluid in a tube with uniform heat flux using a two phase approach, *Int. J. Heat Fluid Fl., vol. 28, pp. 211-219, 2007.*

[21]. Bianco, V., Chiacchio, F., Manca, O., and Nardini, S., Numerical investigation of nanofluids forced convection in circular tubes, Appl. *Therm. Eng., vol. 29, pp. 3632–3642, 2009.*

[22]. Kalteh, M., Abbassi, A., Saffar-Avval, M., and Harting, J., Eulerian–Eulerian two-phase numerical simulation of nanofluid laminar forced convection in a microchannel, *Int. J. Heat Fluid Fl., vol. 32, pp. 107–116, 2011.*

[23]. Kalteh, M., Abbassi, A., Saffar-Avval, M., Frijns, A., Darhuber, A., and Harting, J., Experimental and numerical investigation of nanofluid forced convection inside a wide microchannel heat sink, Appl. *Therm. Eng., vol. 36, pp. 260-268, 2012.*

[24]. Buongiorno, J., Convective transport in nanofluids, *J. Heat Transf., vol.128, pp. 240-250, 2006.*

[25]. Allahyari, S., Behzadmehr, A., and Sarvari, S.M.H., Conjugate heat transfer of laminar mixed convection of a nanofluid through an inclined tube with circumferentially non-uniform heating, *Nanoscale Res. Lett., 6:360, 2011.*

[26]. Sidik, N.A.C., Khakbaz, M., and Jahanshaloo, L., Samion, S., Darus, A.N., Simulation of forced convection in a channel with nanofluid by the Lattice Boltzmann method, *Nanoscale Res. Lett., 8:178, 2013.*

[27]. Wen, D., and Ding, Y., Experimental investigation into convective heat transfer of nanofluids at the entrance region under laminar flow conditions, *Int. J. Heat Mass Tran., vol. 47, pp. 5181–5188, 2004.*

[28]. Heris, S.Z., Esfahany, M.N., and Etemad, S.G., Experimental investigation of convective heat transfer of Al_2O_3/water nanofluid in circular tube, *Int. J. Heat Fluid Fl., vol. 28, pp. 203–210, 2007.*

[29]. He, Y., Jin, Y., Chen, H., Ding, Y., Cang, D., and Lu, H., Heat transfer and flow behaviour of aqueous suspensions of TiO_2 nanoparticles (Nanofluids) flowing upward through a vertical pipe,*Int. J. Heat Mass Tran., vol. 50, pp. 2272–2281, 2007.*

[30]. Ding, Y., Alias, H., Wen, D., and Williams, R.A., Heat transfer of aqueous suspensions of carbon nanotubes (CNT Nanofluids),*Int. J. Heat Mass Tran., vol. 49, pp. 240–250, 2006.*

[31]. Chen, H., Yang, W., He, Y., Ding, Y., Zhang, L., Tan, C., Lapkin, A.A. and Bavykin, D.V., Heat transfer and flow behaviour of aqueous suspensions of titanate nanotubes (Nanofluids), *Powder Technol., vol. 183, pp. 63–72, 2008.*

[32]. Moraveji, M. K., Esmaeili, E., Comparison between single-phase and two-phases CFD modeling of laminar forced convection flow of nanofluids in a circular tube under constant heat flux*, Int. Commun. Heat Mass, vol. 39, pp. 1297–1302, 2012.*

[33]. Nguyen, C.T., Desgranges, F., Roy, G., Galanis, N., Maŕe, T., Boucher, S. and Mintsa, H.A., Temperature and particle-size dependent viscosity data for waterbased nanofluids–hysteresis phenomenon, *Int. J. Heat Fluid Flow, vol. 28, pp. 1492–1506,*

[34]. Shah, R. K., and London, A. L., Laminar forced convection in ducts,Adv. Heat Transfer*, Academic Press, New York, 1978.*